Dyes and Pigments 184 (2021) 108816

Contents lists available at ScienceDirect

Dyes and Pigments

journal homepage: http://www.elsevier.com/locate/dyepig

Fluorescent 1-hydroxy-10-alkylacridin-9(10*H*)-one BF_2-chelates: Large Stokes shift and long emission decay times

Andreas Russegger, Sergey M. Borisov *

Institute of Analytical Chemistry and Food Chemistry, Graz University of Technology, Stremayrgasse 9, 8010, Graz, Austria

ARTICLE INFO

Keywords:
1-Hydroxyacridones
Fluorescence
Synthesis
BF_2-fluorophores

ABSTRACT

New 1-hydroxy-10-alkylacridin-9(10*H*)-one BF_2-chelates absorb in the blue-green part of the electromagnetic spectrum and emit fluorescence with moderate quantum yields of 8–45% in toluene. The dyes show large Stokes shifts about 4300 cm^{-1}, decay times between 5 ns and 15 ns in toluene and high photostabilities. Introduction of a fluorine atom into the acridone cycle results in an increase of the fluorescence quantum yield and decay time whereas immobilization in a rigid polymer matrix (polystyrene) further extends the lifetime up to 18 ns. Large Stokes shifts and long emission decay time make this dye class an interesting platform for time-resolved imaging and sensing applications.

1. Introduction

Fluorescent dyes are widely used in science, technology and daily life (e.g. in high-visibility clothing, optical brighteners or highlighters). Fluorophores are indispensable in biomedical research [1] where numerous dye classes have been applied, for example as probes and labels. Most of them belong to BODIPYs [2,3], difluoroboron β-diketonates [4], xanthenes [5,6], cyanines [7], diketopyrrolopyrroles [8] etc., although also various chromophores of other classes found application in probes based on aggregation-induced emission [9,10].

The potential of fluorescent probes in biomedical applications is often limited by autofluorescence of biological material. Consequently, several strategies have been followed to minimize the interferences caused by autofluorescence, most prominently designing the probes with increased wavelength of excitation and emission [11,12], utilization of upconversion [13,14] or elimination of the background in a time-resolved measurement [15]. The last approach requires emitters with decay time that is significantly longer than that of background fluorescence allowing the latter to decay in the time between the excitation pulse and interrogation of the probe [16]. For instance, in tissues about 90% of background fluorescence has average decay time of 2.5 ns and less than 10% of the intensity belongs to a longer component with the average lifetime of 7.5 ns [17]. Luminescent materials suitable for time-resolved measurements mainly include organic and inorganic afterglow materials with decay times varying from hundreds of milliseconds to seconds [18,19], inorganic lanthanide-based beads [20] (typical decay times from hundreds of μs to several ms), phosphorescent metal complexes with decay times in microsecond time domain [21] and some fluorescent dyes with comparably long decay times (>10 ns and preferably above 15 ns [17]).

One advantage of the fluorescent emitters is that the emission is fairly inert to oxygen quenching, because only emission from the long-lived triplet state is significantly affected by oxygen. Fluorescent dyes also are widely used in fluorescence lifetime imaging microscopy (FLIM) [15] and long decay times are useful for this application as well. Unfortunately, fluorescent emitters with decay times longer than 10 ns are rare [15]; the representatives include (quin)acridones [22], ethidium and propidium halides [23,24], triangulenium dyes [17] [1,3]-dioxolo [4,5-*f*][1,3]benzodioxole esters [25,26], some benzothioxanthenes [27], difluoroboron β-diketonates [4] and acridines [28]. Therefore, search for alternative chromophores with long fluorescence lifetimes remains of high interest.

In addition to long fluorescence lifetime, also large Stokes shifts are favoured for fluorescent emitters. For instance, in intensity-based imaging applications a large Stokes shift reduces the loss of emission light by self-absorption [21] and enables good separation of excitation and emission light.

Acridone is a well-known organic molecule with numerous derivatives reported [29] that find applications for instance as chemotherapeutic agents [30] and anti-malaria drugs [31]. Acridones show fluorescence lifetimes that range from 3 ns to 25 ns and can be modified to couple them to biomolecules [22]. Unfortunately, acridones absorb

* Corresponding author.
E-mail address: sergey.borisov@tugraz.at (S.M. Borisov).

https://doi.org/10.1016/j.dyepig.2020.108816
Received 4 May 2020; Received in revised form 28 August 2020; Accepted 28 August 2020
Available online 2 September 2020

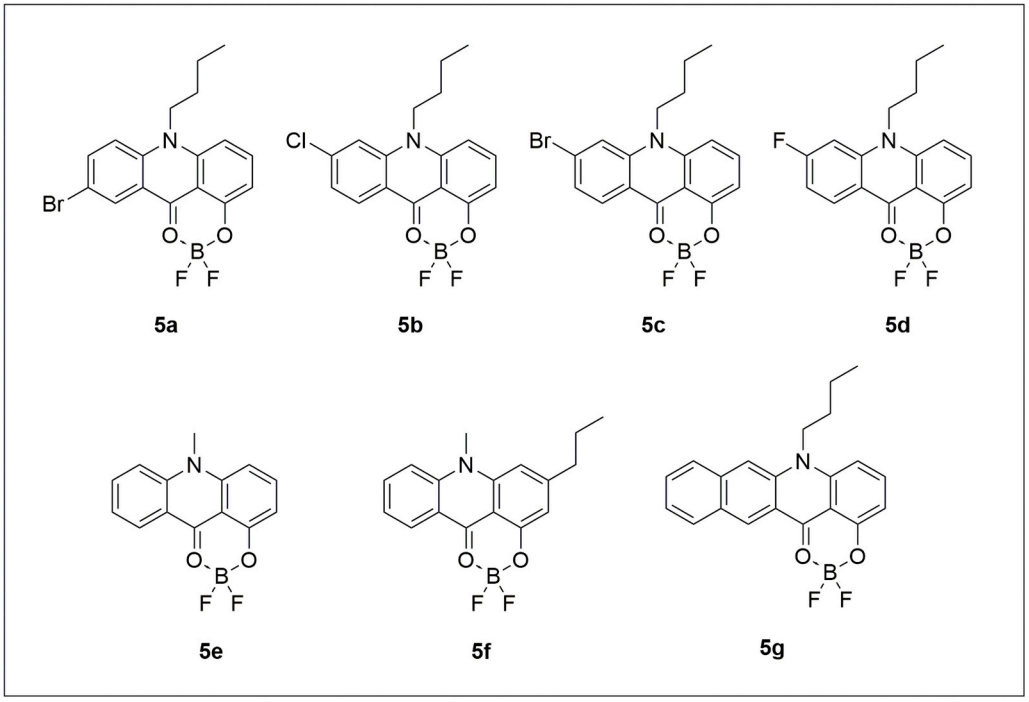

Fig. 1. Structures of the new 1-hydroxy acridone BF_2-chelates.

and emit light in the blue part of the electromagnetic spectrum showing small Stokes shifts. In this work we report a new family of fluorescent dyes, BF_2-chelated 1-hydroxy acridones (Fig. 1), that overcome this drawback featuring large Stokes shifts exceeding 4000 cm^{-1} and retaining up to 15 ns long fluorescence decay times.

2. Experimental section

2.1. Materials

3-Amino-2-naphthoic acid **1,** 5-bromoisatoic anhydride **2a**, 4-chloroisatoic anhydride **2b**, 4-bromoisatoic anhydride **2c**, 4-fluoroisatoic anhydride **2d**, 5-propylcyclohexane-1,3-dione, cyclohexane-1,3-dione were purchased from Fluorochem (www.fluorochem.co.uk), 1-iodobutane (stabilized with copper) was from ABCR (www.abcr.de) and dichloromethane (DCM) was from Fisher scientific (www.fishersci.com). *N*-Methylisatoic anhydride **3e**, dimethyl sulfoxide (DMSO), *N,N*-diisopropylethylamine, bis(trichloromethyl)carbonate and sodium hydride (60% dispersion in paraffin liquid) were purchased from TCI Europe (www.tcichemicals.com). Potassium carbonate, boron trifluoride diethyl etherate (BF_3OEt_2) and tetramethylrhodamine ethyl ester perchlorate (TMR) were obtained from Sigma Aldrich (www.sigmaaldrich.com). Pyridine, acetic acid, dimethylformamide (DMF), tetrahydrofuran (THF, UV/IR grade), toluene (HPLC grade) and anhydrous sodium sulfate were purchased from Carl Roth (www.carlroth.com). Deuterated chloroform ($CDCl_3$), dichloromethane (CD_2Cl_2) and dimethyl sulfoxide (DMSO-D6) were obtained from Eurisotop (www.eurisotop.com) and ethyl acetate (EA), cyclohexane (CH), chloroform ($CHCl_3$), diethyl ether (Et_2O), methanol (MeOH), acetonitrile (ACN), hydrochloric acid (37%) and sodium chloride were from VWR Chemicals (www.vwr.com). Polystyrene (average M.W. 260.000) was obtained from Acros Organics (www.acros.com) and silica gel 60 (0.063–0.200 mm) was from Merk (www.merck.at). Poly(ethylene terephthalate) (PET) support was received from Pütz (www.puetz-folien.com).

2.2. Measurements

^1H and ^{13}C-APT NMR were recorded on a 300 MHz instrument from Bruker (www.bruker.com). The residual signal of the deuterated solvent was used as an internal standard. For data analysis MestReNova NMR-software from Mestrelab (www.mestrelab.com) was used. High resolution mass spectra were recorded on the matrix-assisted laser desorption/ionisation time-of-flight mass spectrometer (MALDI-TOF MS) Micromass MALDI micro MX from Waters (www.waters.com) and on the orthogonal acceleration time-of-flight (oa-TOF) GC mass spectrometer Micromass GCT Premier from Waters. Low resolution mass spectra of the intermediates were acquired on an Expression CMS L compact mass spectrometer from Advion (www.advion.com). The spectrometer was equipped with an APCI (atmospheric-pressure chemical ionisation) ionisation source and quadrupole mass analyser (range 10–2000 *m/z*).

Absorption spectra were recorded on a CARY 50 UV–Vis spectrophotometer from Varian (www.agilent.com). Fluorescence spectra were recorded on a Fluorolog-3 luminescence spectrometer (www.horiba.com) equipped with a NIR-sensitive R2658 photomultiplier from Hamamatsu. Lifetimes were measured using time correlated single photon counting (TCSPC) recorded on the same luminescence spectrometer equipped with a DeltaHub module and a NanoLED excitation source ($\lambda = 453$ nm, pulse duration: 1.1 ns) from Horiba. Data analysis was performed on DAS-6 Analysis software from Horiba using a mono-exponential fit. Absolute quantum yields in toluene and THF were measured on a Fluorolog-3 spectrometer equipped with an integrating sphere Quanta-phi.

The photostability of the dyes **5b**, **5c**, **5f**, **5g** and TMR was evaluated with a previously described home-made set-up that uses a metal-halide lamp as an excitation source [32].

2.3. Preparation of dye-polymer films

Respective dye (0.5 wt% in respect to the polymer) and polystyrene (10 wt% in respect to the solvent) were dissolved in chloroform to obtain a "cocktail". The "cocktails" were knife-coated on a dust-free PET support with a wet film thickness of 75 μm and dried for half an hour at room temperature.

2.4. Synthesis

2*H*-Naphtho[2,3-*d*][1,3]oxazine-2,4(1H)-dione **2g** was synthesized according to literature [33] and 1-hydroxy-10-methylacridin-9 (10H)-one **4e** according to [34].

2.4.1. Synthesis of 5-bromo-N-butylisatoic anhydride (3a)

In a Schlenk tube 5-bromoisatoic anhydride **2a** (1.00 g, 4.13 mmol, 1 eq) was dissolved in dry DMF (15 mL) under argon atmosphere, sodium hydride (170 mg of a 60% NaH dispersion in paraffin liquid, 4.25 mmol, 1.03 eq) was added in one portion and the solution was stirred for 1 h. After 1 h of stirring 1-iodobutane (700 μL, 6.16 mmol, 1.49 eq) was added and stirring continued for 24 h. The solvent was removed under reduced pressure and the brown residue was re-dissolved in the mixture of water (5 mL) and diethyl ether (5 mL). The organic layer was collected and the aqueous layer was extracted twice with diethyl ether. The organic phases were combined, dried over Na_2SO_4 and the solvent was removed under reduced pressure. The product was purified by column chromatography (silica gel) using a gradient from CH to CH:EA (3 + 1) as an eluent and was isolated as a yellow solid (Yield: 676 mg, 55%).

^{1}H NMR (300 MHz, $CDCl_3$) δ 8.26 (d, J = 2.4 Hz, 1H), 7.83 (dd, J = 9.0, 2.4 Hz, 1H), 7.06 (d, J = 8.9 Hz, 1H), 4.03 (t, J = 7.8 Hz, 2H), 1.72 (p, J = 8.1, 7.6 Hz, 2H), 1.46 (h, J = 7.4 Hz, 2H), 0.99 (t, J = 7.3 Hz, 3H). ^{13}C NMR (76 MHz, $CDCl_3$) δ 147.34, 140.50, 140.10, 133.34, 116.73, 115.88, 113.56, 45.16, 28.98, 20.02, 13.83. APCI-MS *m/z*: calc. for: $C_{12}H_{13}BrNO_3$ [MH^+]: 298.0, found: 298.1.

2.4.2. Synthesis of 4-chloro-N-butylisatoic anhydride (3b)

The synthesis of **3b** was performed analogously to **3a**, but 491 mg (2.50 mmol, 1 eq) **2b** dissolved in 10 mL dry DMF, 100 mg (2.50 mmol, 1 eq) sodium hydride (60% dispersion in paraffin liquid) and 430 μL (3.79 mmol, 1.52 eq) 1-iodobutane were used instead. The product was isolated as a white powder (Yield: 365 mg, 58%) by column chromatography (silica gel) using a gradient from CH to CH:EA (3 + 1) as an eluent.

^{1}H NMR (300 MHz, $CDCl_3$) δ 8.09 (d, J = 8.4 Hz, 1H), 7.26 (dd, J = 8.2, 1.5 Hz, 1H), 7.15 (s, 1H), 4.02 (t, J = 7.4 Hz, 2H), 1.73 (p, J = 7.6 Hz, 2H), 1.47 (h, J = 7.3 Hz, 2H), 1.01 (t, J = 7.3 Hz, 3H). ^{13}C NMR (76 MHz, $CDCl_3$) δ 157.82, 147.55, 144.06, 142.44, 132.37, 124.52, 114.30, 110.35, 45.16, 28.94, 20.02, 13.81. APCI-MS *m/z*: calc. for: $C_{12}H_{13}ClNO_3$ [MH^+]: 254.1, found: 254.1.

2.4.3. Synthesis of 4-bromo-N-butylisatoic anhydride (3c)

The synthesis of **3c** was performed analogously to **3a**, but 500 mg (2.07 mmol, 1 eq) **2c** dissolved in 10 mL dry DMF, 82.6 mg (2.07 mmol, 1 eq) sodium hydride (60% dispersion in paraffin liquid) and 350 μL (3.08 mmol, 1.49 eq) 1-iodobutane were used instead. The product was isolated as a white powder (Yield: 261 mg, 42%) by column chromatography (silica gel) using a gradient from CH to CH:EA (10 + 1) as an eluent.

^{1}H NMR (300 MHz, $CDCl_3$) δ 8.00 (d, J = 8.3 Hz, 1H), 7.42 (dd, J = 8.4, 1.6 Hz, 1H), 7.32 (s, 1H), 4.02 (t, J = 7.8 Hz, 2H), 1.73 (p, J = 7.5 Hz, 2H), 1.46 (h, J = 7.4 Hz, 2H), 1.01 (t, J = 7.3 Hz, 3H). ^{13}C NMR (76 MHz, $CDCl_3$) δ 157.98, 154.77, 142.33, 132.70, 132.27, 127.44, 117.26, 110.76, 45.12, 28.95, 20.02, 13.82. APCI-MS *m/z*: calc. for: $C_{12}H_{13}BrNO_3$ [MH^+]: 298.0, found: 297.9.

2.4.4. Synthesis of 4-fluoro-N-butylisatoic anhydride (3d)

The synthesis of **3d** was performed analogously to **3a**, but 498 mg (2.75 mmol, 1 eq) **2d** dissolved in 10 mL dry DMF, 110 mg (2.75 mmol, 1 eq) sodium hydride (60% dispersion in paraffin liquid) and 470 μL (4.14 mmol, 1.5 eq) 1-iodobutane were used instead. The product was isolated as a white powder (Yield: 463 mg, 71%) by column chromatography (silica gel) using a gradient from CH to CH:EA (10 + 1) as an eluent.

^{1}H NMR (300 MHz, $CDCl_3$) δ 8.18 (dd, J = 8.7, 6.2 Hz, 1H), 7.07–6.92 (m, 1H), 6.85 (dd, J = 9.8, 2.0 Hz, 1H), 4.01 (t, J = 7.7 Hz, 2H), 1.73 (p, J = 7.6 Hz, 2H), 1.47 (h, J = 7.3 Hz, 2H), 1.01 (t, J = 7.3 Hz, 3H). ^{13}C NMR (76 MHz, $CDCl_3$) δ 170.07, 166.64, 143.90, 134.16, 134.01, 112.20, 111.89, 108.34, 101.88, 101.51, 45.32, 28.89, 20.03, 13.81. APCI-MS *m/z*: calc. for: $C_{12}H_{13}FNO_3$ [MH^+]: 238.1, found: 237.9.

2.4.5. Synthesis of 1-butyl-2H-naphtho[2,3-d][1,3]oxazine-2,4(1H)-dione (3g)

The synthesis of **3g** was performed analogously to **3a**, but 504 mg (2.36 mmol, 1 eq) **2g** dissolved in 25 mL dry DMF, 95 mg (2.38 mmol, 1 eq) sodium hydride (60% dispersion in paraffin liquid) and 400 μL (3.52 mmol, 1.5 eq) 1-iodobutane were used instead. The product was isolated as a white powder (Yield: 461 mg, 72%) by column chromatography (silica gel) using a gradient from CH to CH + EA (3 + 1) as an eluent.

^{1}H NMR (300 MHz, $CDCl_3$) δ 8.79 (s, 1H), 7.96 (d, J = 8.3 Hz, 1H), 7.87 (d, J = 8.4 Hz, 1H), 7.68 (td, J = 7.0, 1.1 Hz, 1H), 7.53 (t, J = 7.5 Hz, 1H), 7.43 (s, 1H), 4.16 (t, J = 7.8 Hz, 2H), 1.83 (p, J = 7.6 Hz, 2H), 1.53 (h, J = 7.2 Hz, 2H), 1.04 (t, J = 7.3 Hz, 3H). ^{13}C NMR (76 MHz, $CDCl_3$) δ 158.77, 147.49, 137.61, 135.94, 133.81, 130.74, 129.56, 129.01, 127.48, 126.43, 111.57, 110.36, 45.04, 28.66, 20.05, 13.80. APCI-MS *m/z*: calc. for: $C_{16}H_{16}NO_3$ [MH^+]: 270.1, found: 270.0.

2.4.6. Synthesis of 7-bromo-10-butyl-1-hydroxy-10H-acridin-9-one (4a)

Potassium carbonate (96 mg, 0.69 mmol, 1 eq) was suspended in DMSO (15 mL) in a 100 mL round-bottom flask and cyclohexane-1,3-dione (84 mg, 0.75 mmol, 1.1 eq) was added. After stirring the solution for 1 h at room temperature, **3a** (200 mg, 0.67 mmol, 1 eq) was added and the flask was placed in an oil bath (70 °C). The solution was heated to 110 °C over a period of 20 min and was stirred overnight. The dark brown solution was allowed to cool down to room temperature and 1 M HCl (40 mL) was added. The resulting precipitate was collected, washed with water and dried under reduced pressure. The brown solid was purified by column chromatography eluting with 2% MeOH in DCM to get a yellow solid (Yield: 38.4 mg, 11%).

^{1}H NMR (300 MHz, $CDCl_3$) δ 14.24 (s, 1H), 8.51 (d, J = 2.3 Hz, 1H), 7.75 (dd, J = 9.2, 2.3 Hz, 1H), 7.56 (t, J = 8.4 Hz, 1H), 7.33 (d, J = 9.2 Hz, 1H), 6.81 (d, J = 8.7 Hz, 1H), 6.66 (d, J = 8.1 Hz, 1H), 4.25 (t, J = 9.0, 8.1 Hz, 2H), 1.86 (p, J = 7.8 Hz, 2H), 1.64–1.52 (m, 2H), 1.08 (t, J = 7.3 Hz, 3H). ^{13}C NMR (76 MHz, $CDCl_3$) δ 180.92, 163.86, 142.48, 140.43, 137.38, 136.54, 129.42, 122.27, 116.64, 114.85, 110.13, 108.06, 103.68, 46.91, 29.08, 20.27, 13.95. APCI-MS *m/z*: calc. for: $C_{17}H_{17}BrNO_2$ [MH^+]: 346.0, found: 346.1.

2.4.7. Synthesis of 10-butyl-6-chloro-1-hydroxy-10H-acridin-9-one (4b)

The synthesis of **4b** was performed analogously to **4a**, but 109 mg (0.79 mmol, 1 eq) potassium carbonate suspended in 10 mL DMSO, 98 mg (0.84 mmol, 1.1 eq) cyclohexane-1,3-dione and 201 mg (0.79 mmol) **3b** were used instead. The product was isolated as a yellow powder (Yield: 25 mg, 10%) by column chromatography (silica gel) using DCM as an eluent.

^{1}H NMR (300 MHz, $CDCl_3$) δ 14.32 (s, 1H), 8.38 (d, J = 8.6 Hz, 1H), 7.57 (t, J = 8.4 Hz, 1H), 7.43 (s, 1H), 7.22 (d, J = 8.6 Hz, 1H), 6.81 (d, J = 8.7 Hz, 1H), 6.69 (d, J = 8.1 Hz, 1H), 4.22 (t, J = 9.1, 8.4 Hz, 2H), 1.87 (p, J = 7.8 Hz, 2H), 1.59 (h, J = 7.3 Hz, 2H), 1.09 (t, J = 7.3 Hz, 3H). ^{13}C NMR (76 MHz, $CDCl_3$) δ 181.59, 163.98, 142.70, 142.38, 141.25, 136.50, 128.82, 122.28, 119.53, 114.43, 110.16, 108.36, 103.69, 46.89, 29.00, 20.26, 13.94. APCI-MS *m/z*: calc. for: $C_{17}H_{17}ClNO_2$ [MH^+]: 302.1, found: 302.0.

2.4.8. Synthesis of 6-bromo-10-butyl-1-hydroxy-10H-acridin-9-one (4c)

The synthesis of **4c** was performed analogously to **4a**, but 95 mg (0.69 mmol, 1 eq) potassium carbonate suspended in 10 mL DMSO, 81 mg (0.72 mmol, 1.1 eq) cyclohexane-1,3-dione and 199 mg (0.67 mmol) **3c** were used instead. The product was isolated as a yellow powder (Yield: 20 mg, 8.7%) by column chromatography (silica gel) using DCM as an eluent.

^{1}H NMR (300 MHz, $CDCl_3$) δ 14.31 (s, 1H), 8.30 (d, J = 8.8 Hz, 1H),

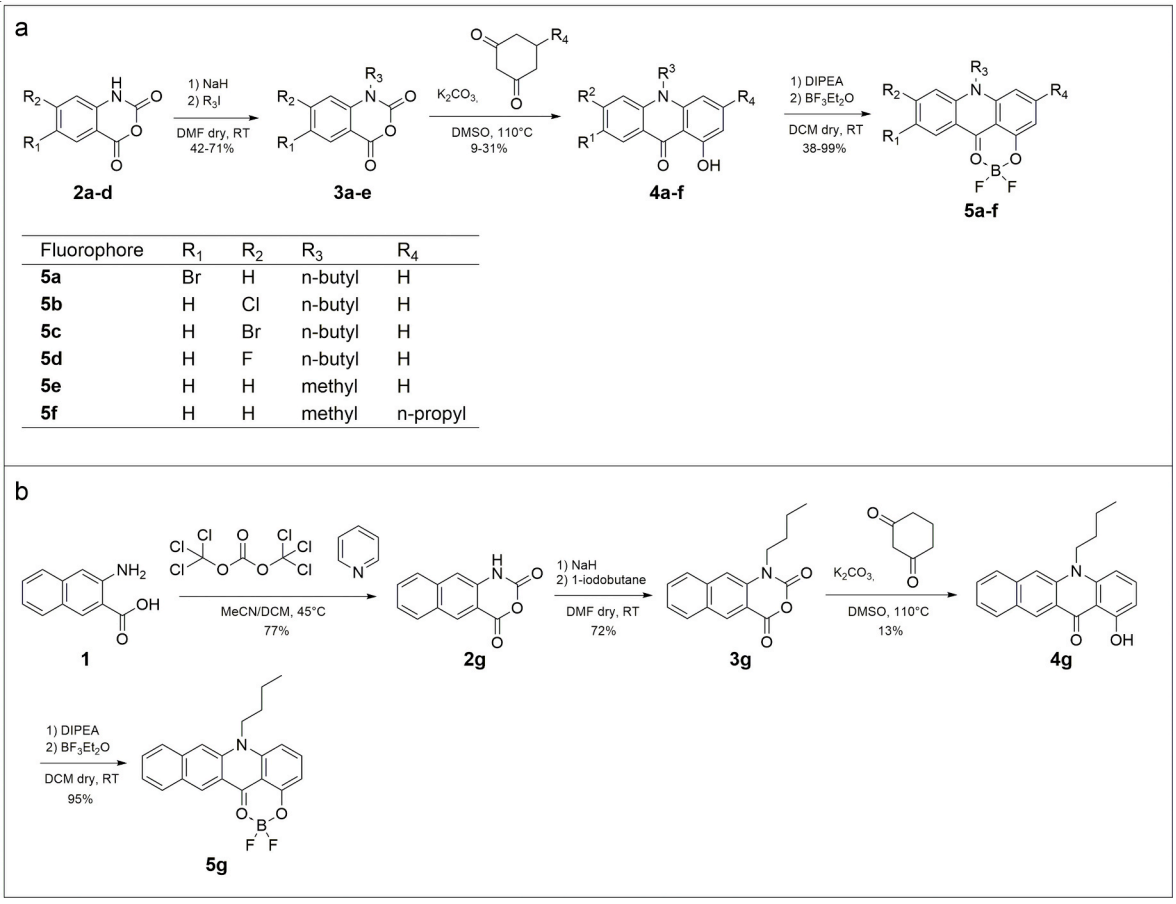

Fluorophore	R_1	R_2	R_3	R_4
5a	Br	H	n-butyl	H
5b	H	Cl	n-butyl	H
5c	H	Br	n-butyl	H
5d	H	F	n-butyl	H
5e	H	H	methyl	H
5f	H	H	methyl	n-propyl

Scheme 1. Overview of the dye synthesis. Synthesis of substituted BF_2-acridone chelates **5a-f** (a) and of the π-extended BF_2-acridone chelate **5g** (b).

7.65–7.52 (m, 2H), 7.37 (dd, J = 8.7, 1.7 Hz, 1H), 6.81 (d, J = 8.6 Hz, 1H), 6.69 (d, J = 8.1 Hz, 1H), 4.23 (t, J = 8.3 Hz, 2H), 1.87 (p, J = 7.6 Hz, 2H), 1.59 (h, J = 8.7, 7.9, 7.3 Hz, 2H), 1.10 (t, J = 7.3 Hz, 3H). ^{13}C NMR (76 MHz, $CDCl_3$) δ 181.73, 163.98, 142.62, 142.41, 136.55, 130.01, 128.76, 125.05, 119.85, 117.50, 110.18, 108.38, 103.71, 46.85, 29.01, 20.25, 13.94. APCI-MS *m/z*: calc. for: $C_{17}H_{17}BrNO_2$ [MH^+]: 346.0, found: 346.1.

2.4.9. Synthesis of 10-butyl-6-fluoro-1-hydroxy-10H-acridin-9-one (4d)

The synthesis of **4d** was performed analogously to **4a**, but 118 mg (0.85 mmol, 1 eq) potassium carbonate suspended in 10 mL DMSO, 104 mg (0.93 mmol, 1.1eq) cyclohexane-1,3-dione and 199 mg (0.84 mmol, 1 eq) **3d** were used instead. The product was isolated as a yellow powder (Yield: 64 mg, 27%) by column chromatography (silica gel) using DCM as an eluent.

^{1}H NMR (300 MHz, $CDCl_3$) δ 14.38 (s, 1H), 8.47 (dd, J = 9.0, 6.8 Hz, 1H), 7.56 (t, J = 8.4 Hz, 1H), 7.09 (dd, J = 11.7, 2.2 Hz, 1H), 7.00 (ddd, J = 9.7, 7.9, 2.2 Hz, 1H), 6.81 (d, J = 8.7 Hz, 1H), 6.69 (d, J = 8.1 Hz, 1H), 4.21 (t, J = 8.4 Hz, 2H), 1.87 (p, J = 8.2, 7.7 Hz, 2H), 1.58 (h, J = 7.4 Hz, 2H), 1.09 (t, J = 7.4 Hz, 3H). ^{13}C NMR (76 MHz, $CDCl_3$) δ 181.47, 168.69, 165.34, 164.06, 143.60, 143.44, 142.90, 136.29, 130.43, 117.93, 110.65, 110.34, 110.00, 108.37, 103.59, 101.02, 100.66, 47.07, 28.91, 20.27, 13.94. APCI-MS *m/z*: calc. for: $C_{17}H_{17}FNO_2$ [MH^+]: 286.1, found: 286.1.

2.4.10. Synthesis of 1-hydroxy-10-methyl-3-propylacridin-9(10H)-one (4f)

The synthesis of **4f** was performed analogously to **4a**, but 157 mg (1.14 mmol, 1 eq) potassium carbonate suspended in 15 mL DMSO, 187 mg (1.21 mmol, 1.1eq) 5-propylcyclohexane-1,3-dione and 200 mg (1.13 mmol, 1 eq) **3e** were used instead. The product was isolated as a yellow powder (Yield: 95 mg, 31%) by column chromatography (silica gel) using 2% MeOH in DCM as an eluent.

^{1}H NMR (300 MHz, $CDCl_3$) δ 14.42 (s, 1H), 8.45 (d, J = 8.0 Hz, 1H), 7.73 (t, J = 8.5 Hz, 1H), 7.50 (d, J = 8.7 Hz, 1H), 7.30 (d, J = 6.9 Hz, 1H), 6.67 (s, 1H), 6.56 (s, 1H), 3.84 (s, 3H), 2.68 (t, J = 7.6 Hz, 2H), 1.76 (h, J = 7.5 Hz, 2H), 1.03 (t, J = 7.3 Hz, 3H). ^{13}C NMR (76 MHz, $CDCl_3$) δ 181.73, 163.51, 152.34, 143.42, 142.45, 134.32, 126.81, 121.41, 121.13, 114.74, 108.44, 108.17, 103.82, 39.54, 34.20, 24.23, 14.03. APCI-MS *m/z*: calc. for: $C_{17}H_{18}NO_2$ [MH^+]: 268.1, found: 268.2.

2.4.11. Synthesis of 5-butyl-1-hydroxybenzo[b]acridin-12(5H)-one (4g)

The synthesis of **4g** was performed analogously to **4a**, but 78 mg (0.56 mmol, 1 eq) potassium carbonate suspended in 10 mL DMSO, 68 mg (0.61 mmol, 1.1eq) cyclohexane-1,3-dione and 151 mg (0.56 mmol, 1 eq) **3g** were used instead. The product was isolated as an orange powder (Yield: 24 mg, 13%) by column chromatography (silica gel) using DCM as an eluent.

^{1}H NMR (300 MHz, $CDCl_3$) δ 14.38 (s, 1H), 9.02 (s, 1H), 7.97 (d, J = 8.3 Hz, 1H), 7.88 (d, J = 8.5 Hz, 1H), 7.73 (s, 1H), 7.64–7.51 (m, 2H), 7.41 (t, J = 7.5 Hz, 1H), 6.79 (d, J = 8.7 Hz, 1H), 6.64 (d, J = 8.1 Hz, 1H), 4.33 (t, J = 8.2 Hz, 2H), 1.95 (p, J = 8.2, 7.6 Hz, 2H), 1.65 (h, J = 7.4 Hz, 2H), 1.13 (t, J = 7.3 Hz, 3H). ^{13}C NMR (76 MHz, $CDCl_3$) δ 183.46, 164.37, 143.64, 138.46, 136.97, 136.93, 129.56, 129.11, 128.56, 128.02, 127.19, 124.88, 121.25, 110.40, 108.77, 107.30, 103.35, 46.78, 28.67, 20.40, 14.05. APCI-MS *m/z*: calc. for: $C_{21}H_{20}NO_2$ [MH^+]: 318.2, found: 318.2.

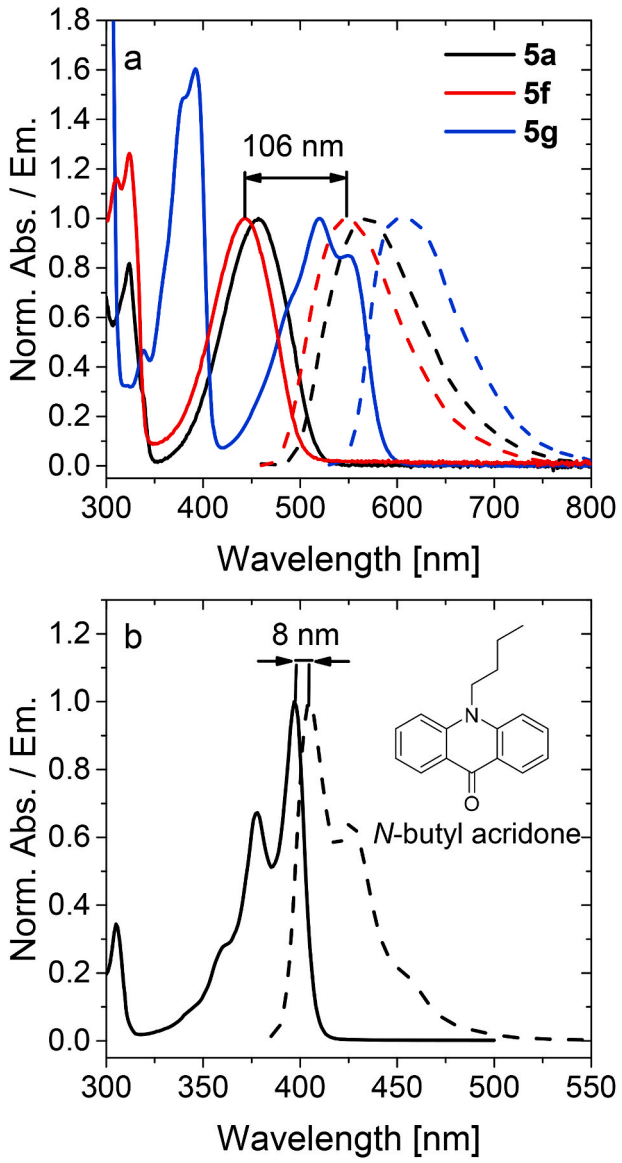

Fig. 2. Normalised absorption (bold lines) and emission spectra (dashed lines) of **5a**, **5f** and **5g** (a) and *N*-butyl acridone in THF (b).

*2.4.12. Synthesis of 7-bromo-10-butyl-1-((difluoroboraneyl)oxy)acridin-9 (10H)-one (**5a**)*

The synthesis was carried out under water-free conditions, under argon atmosphere and shielded from light. **4a** (38 mg, 0.11 mmol, 1 eq) was dissolved in anhydrous DCM (10 ml) and *N*,*N*-diisopropylethylamine (190 μL, 1.12 mmol, 10 eq) was added to the stirred solution. After stirring for 15 min at room temperature boron trifluoride diethyl etherate (200 μL, 1.62 mmol, 15 eq) was added. After another 30 min of stirring the yellow solution was extracted once with an aqueous 1% acetic acid solution and twice with a saturated sodium chloride solution. The organic phase was dried over Na_2SO_4 and the solvent was removed under reduced pressure to yield the product as a yellow solid (Yield: 33 mg, 76%).

^{1}H NMR (300 MHz, CD_2Cl_2) δ 8.83 (d, J = 2.2 Hz, 1H), 8.09 (dd, J = 9.4, 2.3 Hz, 1H), 7.99 (t, J = 8.5 Hz, 1H), 7.73 (d, J = 9.5 Hz, 1H), 7.19 (d, J = 8.9 Hz, 1H), 6.95 (d, J = 8.1 Hz, 1H), 4.71–4.50 (m, 2H), 1.96 (p, J = 7.9 Hz, 2H), 1.63 (h, 7.5 Hz, 2H), 1.08 (t, J = 7.3 Hz, 3H). ^{13}C NMR (76 MHz, CD_2Cl_2) δ 141.61, 140.68, 129.38, 118.12, 110.46, 104.85, 48.61, 29.95, 20.67, 14.04. EI-DI-TOF *m/z*: calc. for: $C_{17}H_{15}BrBF_2NO_2$ [M^+]: 393.0350, found: 393.0344.

*2.4.13. Synthesis of 10-butyl-6-chloro-1-((difluoroboraneyl)oxy)acridin-9 (10H)-one (**5b**)*

The synthesis of **5b** was performed analogously to **5a**, but 25 mg (0.08 mmol, 1 eq) **4b** dissolved in 10 mL dry DCM, 140 μL (0.83 mmol, 10 eq) *N*,*N*-diisopropylethylamine and 150 μL (1.22 mmol, 15 eq) BF_3OEt_2 were used instead. The product was isolated as an orange powder (Yield: 26 mg, 90%).

^{1}H NMR (300 MHz, CD_2Cl_2) δ 8.64 (d, J = 8.8 Hz, 1H), 7.98 (t, J = 8.5 Hz, 1H), 7.83 (d, J = 1.8 Hz, 1H), 7.55 (dd, J = 8.8, 1.7 Hz, 1H), 7.17 (d, J = 8.8 Hz, 1H), 6.96 (d, J = 8.0 Hz, 1H), 4.56 (t, J = 7.7 Hz, 2H), 1.96 (p, J = 7.8 Hz, 2H), 1.64 (h, J = 7.5 Hz, 2H), 1.09 (t, J = 7.3 Hz, 3H). ^{13}C NMR (76 MHz, CD_2Cl_2) δ 141.55, 129.01, 125.43, 115.89, 110.67, 104.84, 48.54, 29.82, 20.65, 14.05. EI-DI-TOF *m/z*: calc. for: $C_{17}H_{15}ClBF_2NO_2$ [M^+]: 349.0856, found: 349.0848.

*2.4.14. Synthesis of 6-bromo-10-butyl-1-((difluoroboraneyl)oxy)acridin-9 (10H)-one (**5c**)*

The synthesis of **5c** was performed analogously to **5a**, but 20 mg (0.06 mmol, 1 eq) **4c** dissolved in 10 mL dry DCM, 100 μL (0.59 mmol, 10 eq) *N*,*N*-diisopropylethylamine and 110 μL (0.89 mmol, 15 eq) BF_3OEt_2 were used instead. The product was further purified by column chromatography (silica gel) using a gradient from CH to CH:EA (4 + 1) as an eluent and was isolated as an orange powder (Yield: 13 mg, 55%).

^{1}H NMR (300 MHz, CD_2Cl_2) δ 8.55 (d, J = 8.8 Hz, 1H), 8.08–7.92 (m, 2H), 7.69 (dd, J = 8.7, 1.5 Hz, 1H), 7.17 (d, J = 8.8 Hz, 1H), 6.96 (d, J = 8.1 Hz, 1H), 4.56 (t, J = 8.4 Hz, 2H), 1.96 (p, J = 8.0 Hz, 2H), 1.64 (h, J = 7.4 Hz, 2H), 1.10 (t, J = 7.3 Hz, 3H). ^{13}C NMR (76 MHz, CD_2Cl_2) δ 141.60, 128.74, 128.13, 119.03, 110.67, 104.86, 48.48, 29.84, 20.64, 14.05. EI-DI-TOF *m/z*: calc. for: $C_{17}H_{15}BrBF_2NO_2$ [M^+]: 393.0350, found: 393.0347.

*2.4.15. Synthesis of 10-butyl-1-((difluoroboraneyl)oxy)-6-fluoroacridin-9 (10H)-one (**5d**)*

The synthesis of **5d** was performed analogously to **5a**, but 18.2 mg (0.06 mmol, 1 eq) **4d** dissolved in 10 mL dry DCM, 110 μL (0.65 mmol) *N*,*N*-diisopropylethylamine and 120 μL (0.97 mmol, 15 eq) BF_3OEt_2 were used instead. The product was further purified by column chromatography (silica gel) using a gradient from CH to CH:EA (4 + 1) as an eluent and was isolated as an orange powder (Yield: 8.1 mg, 38%).

^{1}H NMR (300 MHz, CD_2Cl_2) δ 8.76 (dd, J = 9.2, 6.4 Hz, 1H), 7.98 (t, J = 8.5 Hz, 1H), 7.47 (dd, J = 11.5, 2.2 Hz, 1H), 7.42–7.29 (m, 1H), 7.18 (d, J = 8.8 Hz, 1H), 6.96 (d, J = 8.2 Hz, 1H), 4.53 (t, J = 8.4 Hz, 2H), 1.95 (q, J = 7.9 Hz, 2H), 1.64 (h, J = 7.4 Hz, 2H), 1.09 (t, J = 7.3 Hz, 3H). ^{13}C NMR (76 MHz, CD_2Cl_2) δ 141.10, 130.92, 130.77, 114.39, 114.07, 110.51, 104.56, 102.18, 101.82, 48.54, 29.48, 20.47, 13.86. EI-DI-TOF *m/z*: calc. for: $C_{17}H_{15}BF_3NO_2$ [M^+]: 333.1151, found: 333.1143.

*2.4.16. Synthesis of 1-((difluoroboraneyl)oxy)-10-methylacridin-9(10H)-one (**5e**)*

The synthesis of **5e** was performed analogously to **5a**, but 52 mg (0.23 mmol, 1 eq) **4e** dissolved in 10 mL dry DCM, 300 μL (2.23 mmol, 10 eq) *N*,*N*-diisopropylethylamine and 320 μL (3.32 mmol, 14 eq) BF_3OEt_2 were used instead. The product was isolated as a yellow powder (Yield: 39 mg, 61%).

^{1}H NMR (300 MHz, DMSO) δ 8.53 (d, J = 8.1 Hz, 1H), 8.30 (d, J = 9.0 Hz, 1H), 8.25–8.14 (m, 1H), 8.07 (t, J = 8.4 Hz, 1H), 7.69 (t, J = 7.5 Hz, 1H), 7.60 (d, J = 8.9 Hz, 1H), 6.92 (d, J = 7.9 Hz, 1H), 4.27 (s, 3H).^{13}C NMR (76 MHz, DMSO) δ 157.61, 142.69, 142.35, 140.34, 137.41, 125.10, 124.30, 117.54, 115.23, 108.50, 106.07, 35.80. EI-DI-TOF *m/z*: calc. for: $C_{14}H_{10}BF_2NO_2$ [M^+]: 273.0775, found: 273.0769.

*2.4.17. Synthesis of 1-((difluoroboraneyl)oxy)-10-methyl-3-propylacridin-9(10H)-one (**5f**)*

The synthesis of **5f** was performed analogously to **5a**, but 44 mg

(0.17 mmol, 1 eq) **4f** dissolved in 15 mL dry DCM, 300 μL (1.76 mmol, 10 eq) *N*,*N*-diisopropylethylamine and 320 μL (2.59 mmol, 15 eq) BF_3OEt_2 were used instead. The product was isolated as a yellow powder (Yield: 51 mg, 99%).

^{1}H NMR (300 MHz, DMSO) δ 8.48 (d, J = 8.1 Hz, 1H), 8.24 (d, J = 8.9 Hz, 1H), 8.18–8.08 (m, 1H), 7.64 (t, J = 7.5 Hz, 1H), 7.41 (s, 1H), 6.79 (s, 1H), 4.23 (s, 3H), 2.79 (t, J = 7.5 Hz, 2H), 1.73 (h, J = 7.3 Hz, 2H), 0.96 (t, J = 7.2 Hz, 3H). ^{13}C NMR (76 MHz, DMSO) δ 157.04, 142.56, 142.26, 137.07, 124.99, 124.04, 117.39, 115.11, 109.18, 105.93, 105.58, 35.60, 23.59, 13.71. EI-DI-TOF *m/z*: calc. for: $C_{17}H_{16}BF_2NO_2$ [M^+]: 315.1245, found: 315.1238.

2.4.18. Synthesis of 5-butyl-1-((difluoroboraneyl)oxy)benzo[b]acridin-12 (5H)-one (5g)

The synthesis of **5g** was performed analogously to **5a**, but 11 mg (0.03 mmol, 1 eq) **4g** dissolved in 10 mL dry DCM, 60 μL (0.35 mmol, 10 eq) *N*,*N*-diisopropylethylamine and 65 μL (0.53 mmol, 15 eq) BF_3OEt_2 were used instead. The product was isolated as a red powder (Yield: 12 mg, 95%).

^{1}H NMR (300 MHz, CD_2Cl_2) δ 9.31 (s, 1H), 8.17 (s, 1H), 8.15–8.03 (m, 2H), 7.94 (t, J = 8.4 Hz, 1H), 7.82–7.66 (m, 1H), 7.61–7.49 (m, 1H), 7.11 (d, J = 8.9 Hz, 1H), 6.83 (d, J = 8.1 Hz, 1H), 4.67 (t, J = 8.2 Hz 2H), 2.02 (q, J = 8.4 Hz, 2H), 1.70 (h, J = 7.5 Hz, 2H), 1.13 (t, J = 7.3 Hz, 3H). ^{13}C NMR (76 MHz, CD_2Cl_2) δ 143.60, 142.37, 138.61, 131.27, 129.99, 129.45, 129.22, 128.12, 126.88, 112.63, 109.00, 104.38, 48.19, 29.51, 20.78, 14.15. MALDI-TOF *m/z*: calc. for: $C_{21}H_{18}BF_2NO_2$ [M^+]: 365.1403, found: 365.1407.

3. Result and discussion

3.1. Synthesis of BF_2-1-hydroxyacridone chelates

In this work seven different BF_2-chelates with various substitution patterns (Fig. 1) were synthesized and characterised. The synthesis of the chelates **5a-d** was performed in three steps (Scheme 1), starting with the isatoic anhydride derivatives **2a-d** and the compounds **5e** and **5f** in two steps, starting from the commercially available *N*-methylisatoic anhydride **3e**. In case of the π-extended **5g** a fourth synthetic step was necessary to get the isatoic anhydride **2g** from 3-amino-2-naphthoic acid **1** according to literature [33].

In order to render the dyes soluble in organic solvents an alkyl substituent was introduced. The isatoic anhydride derivatives **2a-2d** and **2g** were converted to the N-substituted isatoic anhydride derivatives **3a-3d** and **3g** by the reaction with butyl iodide in the presence of sodium hydride in moderate yields. Then, **3a-e** and **3g** were condensed with the potassium salt of either cyclohexane-1,3-dione or 5-propylcyclohexane-1,3-dione at 110 °C to give 1-hydroxyacridones **4a-g**. This reaction was performed according to previously described method [34]. In the last step **4a-g** were chelated with BF_3Et_2O in presence of *N*,*N*-diisopropylethylamine to the final compounds **5a-g**. The structures of the chelates were confirmed by high-resolution EI-DI-TOF and MALDI-TOF MS and ^{1}H- and ^{13}C-APT-NMR (Supporting information). Unfortunately, due to fairly low solubility of the complexes, no signals corresponding to quaternary carbons were observed in the ^{13}C-APT-NMR spectra.

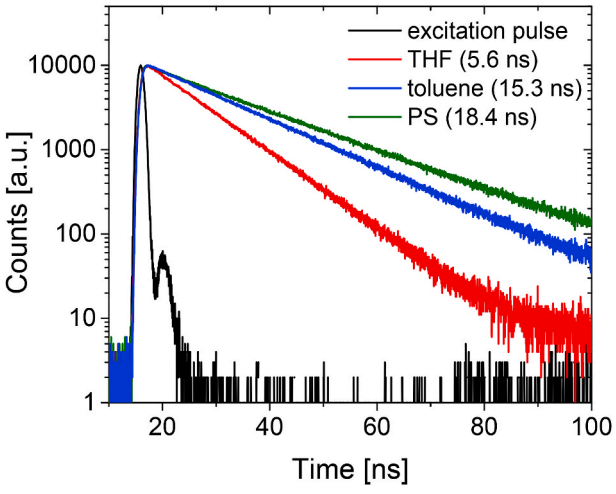

Fig. 3. Luminescence decays for **5d** measured in different media.

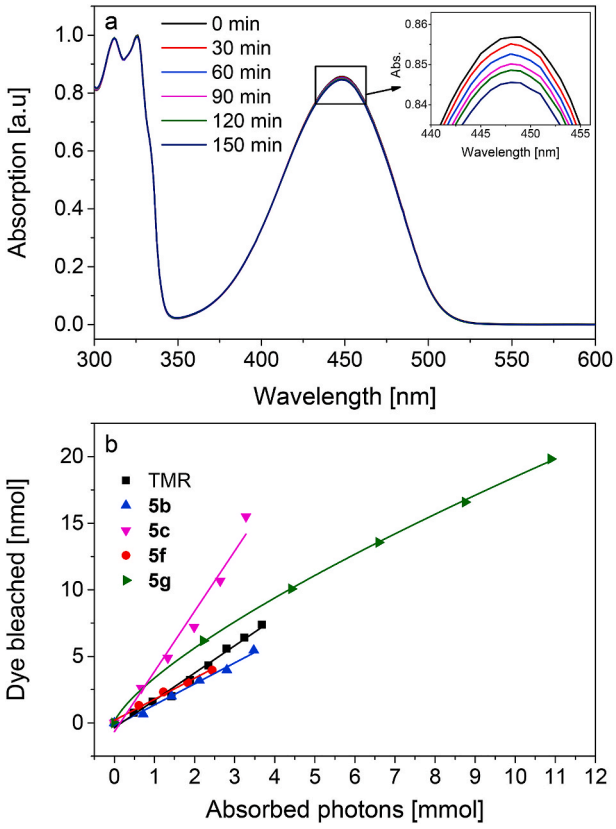

Fig. 4. Absorption spectra during irradiation of solution of **5b** in THF with the light of metal-halogen lamp (a) and photodegradation of fluorophores and the reference dye TMR in the same conditions (b).

3.2. Photophysical properties

Absorption and emission spectra of three representatives (**5a, 5f** and **5g)** are depicted in Fig. 2a. The spectra for all the dyes are shown in the supporting information (Fig. S1). The fluorophores show broad absorption and emission bands (FWHM ~ 3500-3900 cm^{-1}). Halide substituents have a minor effect on the position of absorption and emission bands: the spectra shift bathochromically in the row **5d** (F) – **5e** (H) – **5b** (Cl) – **5c** (Br). It should be noted that the alkyl substituent in case of **5e** and other dyes is not identical (methyl and butyl, respectively). Among the brominated derivatives, **5a** (substituent in the 7-position) absorbs and emits at longer wavelength than **5c**, bearing Br in the 6-position. As expected, the extension of π-system in case of **5g** results in much stronger bathochromic shift of the absorption (74 nm compared to **5e**) and emission (47 nm compared to **5e**) spectra. An important feature of the new dyes is their large Stokes shift (>4200 cm^{-1} for **5a-5f**, but 2510 cm^{-1} for **5g**) that significantly exceed that typical for the BODIPY chromophores (<1300 cm^{-1} for most representatives) [35]. The Stokes shift is however comparable to that shown by curcuminoid-based difluoroboron β-diketonates [36–39]. The large Stokes shift enables almost complete separation of the excitation and emission which is

Table 1
Photophysical properties of the BF_2-acrdione complexes. Absorption maxima (λ_{abs}), molar absorption coefficients (ε), emission maxima (λ_{em}) in THF, fluorescence lifetimes (τ) and quantum yields (Φ).

Dye	λ_{abs} [nm]	ε [M^{-1} cm^{-1}]	λ_{em} [nm]	Stokes shift [cm^{-1}]	τ_{THF} [ns]	$\tau_{toluene}$ [ns]	Φ_{THF} [%]	$\Phi_{toluene}$ [%]
5a	457	4880	570	4340	2.7	4.9	4	8
5b	449	6180	556	4290	5.1	10.5	7	21
5c	449	7060	560	4410	3.6	5.6	5	11
5d	439	7030	542	4330	9.6	15.3	20	45
5e	446	6730	551	4270	7.2	12.6	12	31
5f	443	5790	549	4360	7.1	12.2	11	23
5g	392, 520	8500, 5330	598	2510	3.3	7.3	6	16

useful in many applications, like intensity-based imaging. Introduction of bromine (**5a** and **5c**) decreases the fluorescence quantum yield in toluene by about 4-fold in comparison to the unsubstituted **5e** (Table 1), which may be caused by enhancement of inter-system crossing due to the heavy atom effect [40]. Substitution with a chlorine atom (**5b**) also leads to reduction of the quantum yield, albeit much smaller compared to bromine substitution (Table 1). Similar effects were observed for other molecules, like phenanthrene [41]. In contrast, a fluorine atom introduced in the same position (**5d**) enhances the fluorescence quantum yield by about 1.5-fold compared to the unsubstituted parent compound (**5e**).

It is interesting to compare the spectral properties of the new dye with those of *N*-alkyl-substituted acridone. As can be seen (Fig. 2b), acridone absorbs in the UV part of the electromagnetic spectrum and emits blue light, showing small Stokes shift of only 8 nm. The introduction of OH-substituent and subsequent formation of the BF_2-chelates leads to a stronger charge transfer character of the molecule. Such change is manifested in significant bathochromic shift of the absorption spectra (~50 nm) and even much stronger shift (~140 nm) of the emission compared to the parent acridone as well as in characteristic large Stokes shift.

Fluorescence decays are exemplified for **5d** in Fig. 3 and the obtained decay times for all the dyes are compiled in Table 1. As can be seen, the fluorescence decay times strongly depend on the nature of substituents and the solvent. The decay times follow the trend observed for the fluorescence quantum yield with bromo-substituted derivatives **5a** and **5c** having the shortest decay times and fluoro-substituted **5d** the longest, whereas the chelates bearing no halide atoms occupy intermediate position. For all the dyes, the decay times are shorter in more polar THF compared to toluene (Table 1). **5d** dissolved in toluene shows rather long fluorescence decay time of 15.3 ns that is comparable to those of triangulenium and [1,3]dioxolo[4,5*f*][1,3]benzodioxole ester chromophores. Immobilization in a rigid matrix (polystyrene) results in further increase of the fluorescence lifetime to 18.4 ns. Notably, the fluorescence decay times of the π-extended derivative **5g** are much shorter and are similar to those observed for most fluorescent dyes.

The photostability of four dyes was evaluated by irradiating their solutions in THF with the polychromatic light of a metal-halide lamp (narrowed to 400–700 nm with help of filters) and monitoring the absorption (Fig. 4a). As can be seen, the photostability of **5b**, **5c** and **5f** is generally similar to that of the commercially available tetramethylrhodamine (TMR). For instance, the photobleaching quantum yield Φ_{bl} for **5b** calculated from the slope of the plot presented in Fig. 4b is 1.6×10^{-6}. In other words, the chromophore survives in average $1/\Phi_{bl} = 6.3 \times 10^5$ excitation cycles. Notably, the bromo-substituted **5c** shows faster photodegradation ($\Phi_{bl} = 4.5 \times 10^{-6}$) possibly due to enhanced population of the triplet state and further generation of reactive species such as singlet oxygen. In contrast to the other investigated dyes, photobleaching of **5g** appears to be faster in the beginning which might be due to multiple photobleaching pathways e.g. involving impurities in the solvent that get consumed during the experiment.

4. Conclusions

In conclusion, new BF_2-chelates of 1-hydroxy-10-alkylacridin-9(10*H*)-one represent an interesting class of fluorophores that show very large Stokes shifts and, in case of some representatives, long fluorescence lifetimes. Among the new compounds, the fluorinated derivative shows the best photophysical properties with the highest fluorescence quantum yield and the longest decay time that is comparable to the fluorescence lifetimes of triangulenium and [1,3]dioxolo[4,5-*f*][1,3]benzodioxole ester dyes. The synthesis of the new dyes is straightforward allowing further synthetic modifications to introduce various substituents that: (i) may further enhance the photophysical properties (for instance several additional fluorine substituents); (ii) modulate the fluorescence properties in presence of different analytes and (iii) enable covalent coupling of the dyes to biomolecules.

Declaration of competing interest

The authors declare that they have no known competing financial interests or personal relationships that could have appeared to influence the work reported in this paper.

Acknowledgements

The support from Ing. Karin Bartl (ICTM, TU Graz) in the acquisition of the MS-Spectra is gratefully acknowledged. This research did not receive any specific grant from funding agencies in the public, commercial, or not-for-profit sectors.

Appendix A. Supplementary data

Supplementary data to this article can be found online at https://doi.org/10.1016/j.dyepig.2020.108816.

References

[1] Lavis LD, Raines RT. Bright ideas for chemical biology. ACS Chem Biol 2008;3:142–55. https://doi.org/10.1021/cb700248m.
[2] Boens N, Leen V, Dehaen W. Fluorescent indicators based on BODIPY. Chem Soc Rev 2012;41:1130–72. https://doi.org/10.1039/c1cs15132k.
[3] Kowada T, Maeda H, Kikuchi K. BODIPY-based probes for the fluorescence imaging of biomolecules in living cells. Chem Soc Rev 2015;44:4953–72. https://doi.org/10.1039/c5cs00030k.
[4] Chen PZ, Niu LY, Chen YZ, Yang QZ. Difluoroboron β-diketonate dyes: Spectroscopic properties and applications. Coord Chem Rev 2017;350:196–216. https://doi.org/10.1016/j.ccr.2017.06.026.
[5] Wang L, Du W, Hu Z, Uvdal K, Li L, Huang W. Hybrid rhodamine fluorophores in the visible/NIR region for biological imaging. Angew Chem Int Ed 2019;58:14026–43. https://doi.org/10.1002/anie.201901061.
[6] Chen X, Pradhan T, Wang F, Kim JS, Yoon J. Fluorescent chemosensors based on spiroring-opening of xanthenes and related derivatives. Chem Rev 2012;112:1910–56. https://doi.org/10.1021/cr200201z.
[7] Sun W, Guo S, Hu C, Fan J, Peng X. Recent development of chemosensors based on cyanine platforms. Chem Rev 2016;116:7768–817. https://doi.org/10.1021/acs.chemrev.6b00001.
[8] Li W, Wang L, Tang H, Cao D. Diketopyrrolopyrrole-based fluorescent probes for detection and bioimaging: Current progresses and perspectives. Dyes Pigments 2019;162:934–50. https://doi.org/10.1016/j.dyepig.2018.11.023.

[9] Zhang X, Zhang X, Tao L, Chi Z, Xu J, Wei Y. Aggregation induced emission-based fluorescent nanoparticles: Fabrication methodologies and biomedical applications. J Mater Chem B 2014;2:4398–414. https://doi.org/10.1039/c4tb00291a.
[10] Ding D, Li K, Liu B, Tang BZ. Bioprobes based on AIE fluorogens. Acc Chem Res 2013;46:2441–53. https://doi.org/10.1021/ar3003464.
[11] Hong G, Antaris AL, Dai H. Near-infrared fluorophores for biomedical imaging. Nat Biomed Eng 2017;1:1–22. https://doi.org/10.1038/s41551-016-0010.
[12] Escobedo JO, Rusin O, Lim S, Strongin RM. NIR dyes for bioimaging applications. Curr Opin Chem Biol 2010;14:64–70. https://doi.org/10.1016/j.cbpa.2009.10.022.
[13] Chen G, Qiu H, Prasad PN, Chen X. Upconversion nanoparticles: design, nanochemistry, and applications in Theranostics. Chem Rev 2014;114:5161–214. https://doi.org/10.1021/cr400425h.
[14] Chatterjee DK, Gnanasammandhan MK, Zhang Y. Small upconverting fluorescent nanoparticles for biomedical applications. Small 2010;6:2781–95. https://doi.org/10.1002/smll.201000418.
[15] Berezin MY, Achilefu S. Fluorescence lifetime measurements and biological imaging. Chem Rev 2010;110:2641–84. https://doi.org/10.1021/cr900343z.
[16] Zhang KY, Yu Q, Wei H, Liu S, Zhao Q, Huang W. Long-lived emissive probes for time-resolved photoluminescence bioimaging and biosensing. Chem Rev 2018;118:1770–839. https://doi.org/10.1021/acs.chemrev.7b00425.
[17] Rich RM, Stankowska DL, Maliwal BP, Sørensen TJ, Laursen BW, Krishnamoorthy RR, et al. Elimination of autofluorescence background from fluorescence tissue images by use of time-gated detection and the AzaDiOxaTriAngulenium (ADOTA) fluorophore. Anal Bioanal Chem 2013;405:2065–75. https://doi.org/10.1007/s00216-012-6623-1.
[18] Xu S, Chen R, Zheng C, Huang W. Excited state modulation for organic afterglow: materials and applications. Adv Mater 2016;28:9920–40. https://doi.org/10.1002/adma.201602604.
[19] Liang L, Chen N, Jia Y, Ma Q, Wang J, Yuan Q, et al. Recent progress in engineering near-infrared persistent luminescence nanoprobes for time-resolved biosensing/bioimaging. Nano Res 2019;12:1279–92. https://doi.org/10.1007/s12274-019-2343-6.
[20] Cai H, Fujimoto K, Lim JM, Wang C, Huang W, Rao Y, et al. Synthesis of direct β-to-β linked porphyrin arrays with large electronic interactions: Branched and cyclic oligomers. Angew Chem Int Ed 2014;53:11088–91. https://doi.org/10.1002/anie.201407032.
[21] Baggaley E, Weinstein JA, Williams JAG. Lighting the way to see inside the live cell with luminescent transition metal complexes. Coord Chem Rev 2012;256:1762–85. https://doi.org/10.1016/j.ccr.2012.03.018.
[22] Smith JA, West RM, Allen M. Acridones and quinacridones: Novel fluorophores for fluorescence lifetime studies. J Fluoresc 2004;14:151–71. https://doi.org/10.1023/B:JOFL.0000016287.56322.eb.
[23] Cui HH, Valdez JG, Steinkamp JA, Crissman HA. Fluorescence lifetime-based discrimination and quantification of cellular DNA and RNA with phase-sensitive flow cytometry. Cytometry 2003;52:46–55. https://doi.org/10.1002/cyto.a.10022.
[24] Burns VWF. Fluorescence decay time characteristics of the complex between ethidium bromide and nucleic acids. Arch Biochem Biophys 1969;133:420–4. https://doi.org/10.1016/0003-9861(69)90471-8.
[25] Wessig P, Wawrzinek R, Möllnitz K, Feldbusch E, Schilde U. A new class of fluorescent dyes based on 1,3-benzodioxole and [1,3]-dioxolo[4.5-f]benzodioxole. Tetrahedron Lett 2011;52:6192–5. https://doi.org/10.1016/j.tetlet.2011.09.058.
[26] Schwarze T, Mertens M, Müller P, Riemer J, Wessig P, Holdt HJ. Highly K+-Selective fluorescent probes for lifetime sensing of K+ in living cells. Chem Eur J 2017;23:17186–90. https://doi.org/10.1002/chem.201703799.
[27] Andrés Castán JM, Abad Galán L, Li S, Dalinot C, Simón Marqués P, Allain M, et al. Nitration of benzothioxanthene: towards a new class of dyes with versatile photophysical properties. New J Chem 2020;44:900–5. https://doi.org/10.1039/c9nj05804d.
[28] Maltman BA, Dunsmore CJ, Couturier SCM, Tirnaveanu AE, Delbederi Z, McMordie RAS, et al. 9-Aminoacridine peptide derivatives as versatile reporter systems for use in fluorescence lifetime assays. Chem Commun 2010;46:6929–31. https://doi.org/10.1039/c0cc01901a.
[29] Acheson RM. Chemistry of Heterocyclic compounds. Hoboken, NJ, USA: John Wiley & Sons, Inc.; 1973. https://doi.org/10.1002/9780470186596.
[30] Belmont P, Bosson J, Godet T, Tiano M. Acridine and acridone derivatives, anticancer properties and synthetic methods: where are we now? Anticancer Agents Med Chem 2008;7:139–69. https://doi.org/10.2174/187152007780058669.
[31] Basco LK, Mitaku S, Skaltsounis AL, Ravelomanantsoa N, Tillequin F, Koch M, et al. In vitro activities of furoquinoline and acridone alkaloids against Plasmodium falciparum. Antimicrob Agents Chemother 1994;38:1169–71. https://doi.org/10.1128/aac.38.5.1169.
[32] Pfeifer D, Russegger A, Klimant I, Borisov SM. Green to red emitting BODIPY dyes for fluorescent sensing and imaging of carbon dioxide. Sensor Actuator B Chem 2020;304. https://doi.org/10.1016/j.snb.2019.127312.
[33] Liang JL, Park SE, Kwon Y, Jahng Y. Synthesis of benzo-annulated tryptanthrins and their biological properties. Bioorg Med Chem 2012;20:4962–7. https://doi.org/10.1016/j.bmc.2012.06.034.
[34] Coppola GM. A one-step synthesis of 1-hydroxy-10-methyl-9(10H)-acridinone. Org Prep Proced Int 1999;31:225–7. https://doi.org/10.1080/00304949909355719.
[35] Ulrich G, Ziessel R, Harriman A. The chemistry of fluorescent bodipy dyes: Versatility unsurpassed. Angew Chem Int Ed 2008;47:1184–201. https://doi.org/10.1002/anie.200702070.
[36] Bai G, Yu C, Cheng C, Hao E, Wei Y, Mu X, et al. Syntheses and photophysical properties of BF2 complexes of curcumin analogues. Org Biomol Chem 2014;12:1618–26. https://doi.org/10.1039/c3ob42201a.
[37] Zhang X, Tian Y, Li Z, Tian X, Sun H, Liu H, et al. Design and synthesis of curcumin analogues for in vivo fluorescence imaging and inhibiting copper-induced cross-linking of amyloid beta species in alzheimer's disease. J Am Chem Soc 2013;135:16397–409. https://doi.org/10.1021/ja405239v.
[38] Chongzhao R, Xiaoyin X, Raymond SB, Ferrara BJ, Neal K, Bacskai BJ, et al. Design, synthesis, and testing of difluoroboron-derivatized curcumins as near-infrared probes for in vivo detection of amyloid-β deposits. J Am Chem Soc 2009;131:15257–61. https://doi.org/10.1021/ja9047043.
[39] Kamada K, Namikawa T, Senatore S, Matthews C, Lenne PF, Maury O, et al. Boron difluoride curcuminoid fluorophores with enhanced two-photon excited fluorescence emission and versatile living-cell imaging properties. Chem Eur J 2016;22:5219–32. https://doi.org/10.1002/chem.201504903.
[40] Bolton O, Lee K, Kim HJ, Lin KY, Kim J. Activating efficient phosphorescence from purely organic materials by crystal design. Nat Chem 2011;3:205–10. https://doi.org/10.1038/nchem.984.
[41] Masetti F, Mazzucato U, Galiazzo G. Heavy atom effect on the luminescence of phenanthrene. J Lumin 1971;4:8–12. https://doi.org/10.1016/0022-2313(71)90003-2.